Transport and Communications Science Journal

LONGITUDINAL STRAIN ANALYSIS IN ASPHALT PAVEMENT UNDER FULL-SCALE MOVING LOADS

Le Xuan Quy[1,2*], Nguyen Mai Lan[1], Nguyen Quang Tuan[2], Hornych Pierre[1]

[1]MAST-LAMES, Gustave Eiffel University, Nantes, France

[2]University of Transport and Communications, No 3 Cau Giay Street, Hanoi, Vietnam

ARTICLE INFO

TYPE: Research Article
Received: 19/10/2021
Revised: 29/11/2021
Accepted: 17/02/2022
Published online: 15/05/2022
https://doi.org/10.47869/tcsj.73.4.2

[*] *Corresponding author*
Email: lexuanquy@utc.edu.vn; Tel: 0977939186

Abstract. T The roadway networks have been played a vital role in the development of all countries. The assessments of pavement conditions during their service life are therefore decisive to maintain the stable performance of the network. From this point of view, pavement instrumentation allows monitoring pavement conditions continuously and without traffic interruption. The study aims to illustrate the effectiveness of embedded strain gauges and temperature probes to follow the pavement responses with different traffic speeds, traffic loads and temperature conditions. The longitudinal strain signals are then examined with regards to representative parameters of the loading times and strain amplitude. The results show that the traffic load levels and asphalt temperature are directly responsible for the change of strain amplitudes, while those have almost no impact on loading times. Numerical simulations are also introduced to validate the applicability of both layered elastic and viscoelastic models to the strain signals observed in the field.

Keywords: longitudinal strain, instrumentation, accelerated full-scale experiment, strain signal.

1. INTRODUCTION

The horizontal tensile strain at the bottom of asphalt layers has been a critical parameter in pavement design in many countries [1–3]. As the leading cause of the asphalt pavement damage under the effect of traffic solicitations and environmental conditions, high tensile

asphalt strain levels have become significant interest in recent decades [4–6]. The knowledge of asphalt strain of the in-situ pavement, therefore, is a key element to govern and ensure the quality and performance of the pavement during its service life as proposed in the study of Shafiee et al. [7], Yoo et al. [8], Al-Qadi [9] among others.

The objective of the study is to illustrate the strain measurement in the instrumented asphalt pavement with the changes of loading solicitations (traffic load levels and speeds) and asphalt temperature. To achieve that goal, strain and temperature instrumentations were carried out on the accelerated pavement testing facility (APT) at Nantes campus, Gustave Eiffel University, France. The pavement was then applied to different traffic configurations to serve as the study of pavement response. Detailed representations of longitudinal strain signals were then presented to point out the effect of traffic solicitations and temperature on asphalt strain. The last part is the modelling of the pavement response using elastic (Alize) and viscoelastic (ViscoRoute) multilayer programs. The experimental strain signal at the non-damage stage is then compared to the simulations to assess the simulation accuracy of the two models.

2. MATERIALS, PAVEMENT STRUCTURE AND TEST PROGRAM

2.1. Pavement structure and asphalt concrete material

Pavement structure

The experimental test track has a 19-meter length was constructed with the pavement structure of two asphalt layers (AC), an unbound granular material (UGM) subbase and one soil layer (see Figure 1). The semi-coarse asphalt concrete (SCAC) 0/10 mm (the maximum aggregate size) of class 3 [10] with the binder made of a neat bitumen of 35/50 penetration grade [11] was used for both two asphalt layers. The binder content is 5.58% by mass of the aggregate. The bearing capacity of the soil layer, measured during the construction by dynamic load plate tests [12], was between 95 and 110 MPa. The UGM layer modulus, measured during the construction by dynamic load plate tests, was between 150-200 MPa. The stiffness modulus of the asphalt mixture was approximately 12 000 MPa at 15°C and 10 Hz, obtained from the two-point bending tests [13] which were carried out on samples extracted during the construction.

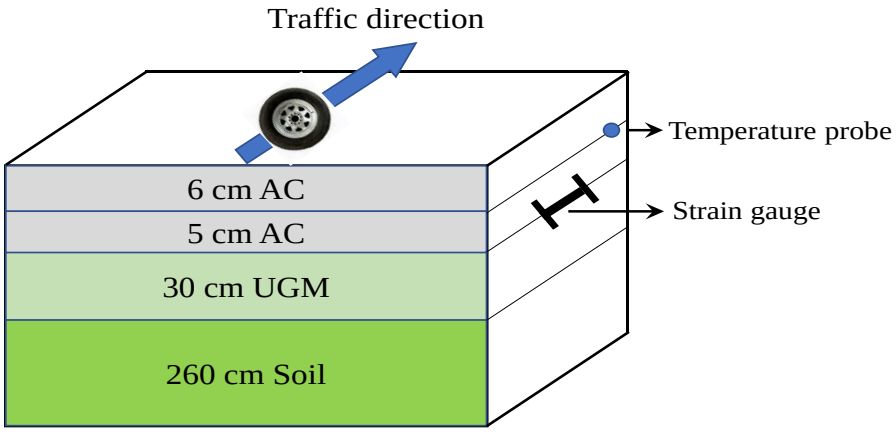

Figure 1. Pavement structure and instrumentation layout.

Complex modulus of asphalt mixture

Complex modulus tests were performed on the asphalt mixture in the laboratory. The test results are presented in Figure 2. The Cole-Cole plan (Figure 2a) illustrates the relationship between the real (E_1) and the imaginary (E_2) components of the complex modulus of bituminous material, while the Black space (Figure 2b) plots $|E^*|$ values against the corresponding phase angle values. It can be seen that there is an existence of a unique curve in both graphs that verifies the application of the Time-Temperature Superposition Principle – TTSP [14,15] to construct a master curve from isothermal curves in Figure 3.

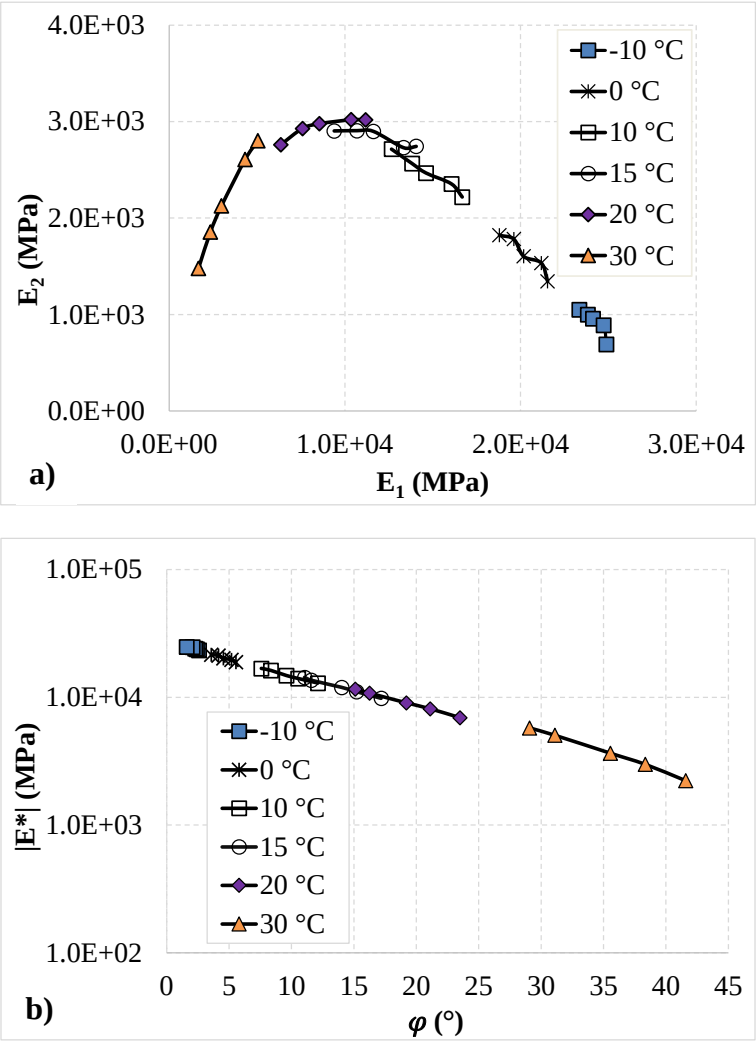

Figure 2. Curves of the complex modulus in the: a) Cole-Cole plan, and b) Black space.

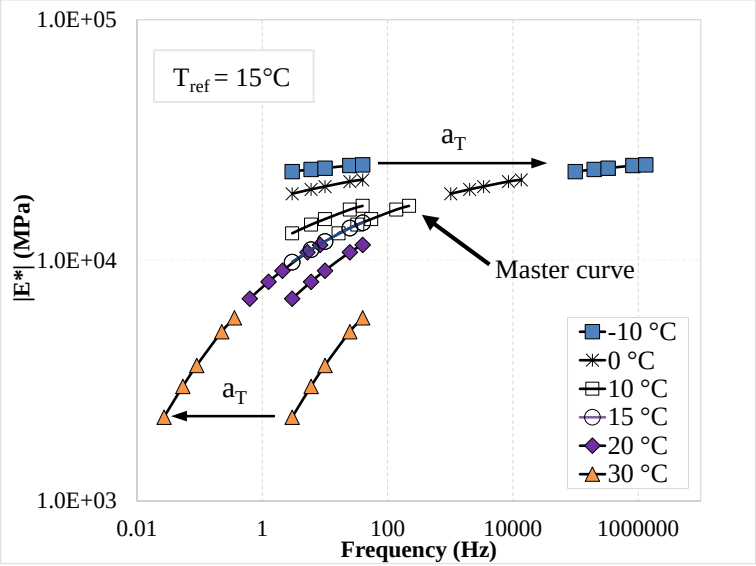

Figure 3. The master curve of complex modulus as a function of frequency at reference temperature of 15°C.

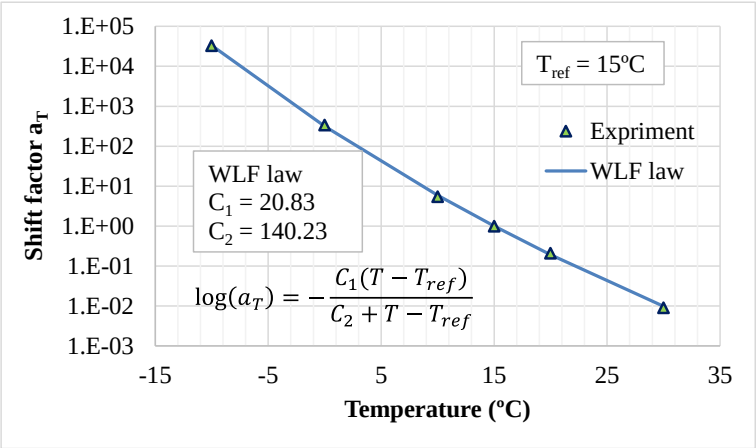

Figure 4. The shift factors (a_T) obtained during the construction of the complex modulus master curve and the WLF law.

The master curve, in Figure 3, is established by shifting parallel each isothermal curve to the frequency axis with the shift factor a_T at the reference temperature of 15°C. The shift factor a_T (Figure 4) is calibrated using the WLF law [16]. It is then possible to obtain asphalt complex modulus values for inaccessible frequencies in the experiment.

2.2. Test program

The study is a part of the fatigue experiment, at which the traffic solicitations were produced by a one thousand horse-power electro-hydraulic facility (Figure 5), with a central tower and four 19-metre loading arms which can generate traffic load up to 150 kN at a maximum speed of 100 km/h [17–19]. At the end of the fatigue experiment, a total of 2.2 million cycles of the equivalent 65 kN dual wheel load was applied.

Figure 5. View of the accelerated pavement testing facility at Gustave Eiffel University, France [20].

Longitudinal strain gauges (KM-100HAS model, see Figure 6) were instrumented at the bottom of the asphalt layers to monitor the pavement responses under the full-scale traffic loads at different traffic speeds.

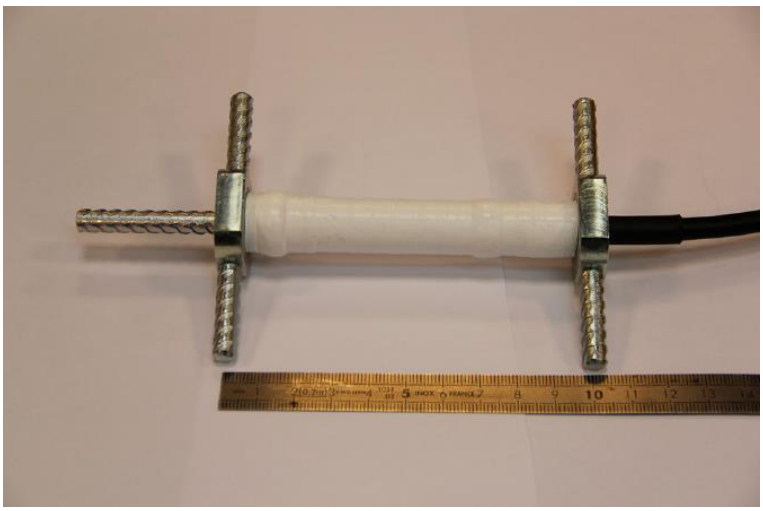

Figure 6. Strain gauge, type KM-100HAS, for the strain measurement in asphalt layers [18].

The results presented in this paper were during the first approximately 50 000 equivalent 65 kN load cycles when it was assumed that no damage happened to the pavement. In this phase, the traffic was controlled at three load levels of 45, 55, and 65 kN and at speeds of 7, 14, 21, 29, 43, 57, and 72 km/h. Asphalt strain was recorded corresponding to different configurations of traffic load levels and speeds. The temperature data was obtained for each 10 minutes thanks to an embedded temperature probe at the depth of 6 cm in asphalt layers, providing precise temperature data to each strain measurement moment.

3. LONGITUDINAL STRAIN ANALYSIS

3.1. Characteristics of a longitudinal strain signal

Figure 7 introduces a characteristic longitudinal strain signal at the bottom of the base asphalt layer in the experimental pavement. As the traffic load moves close to the strain gauge

position, a contraction pick (1) is observed (negative value in longitudinal strain). Following tension pick (3) appears when the load is right on the strain gauge (positive value in longitudinal strain). When the load passes the position of the strain gauge, the signal will move to the second contraction pick (5). Between the two contraction picks and tension pick, two zero points (2,4) are identified when strain values are equal to zero.

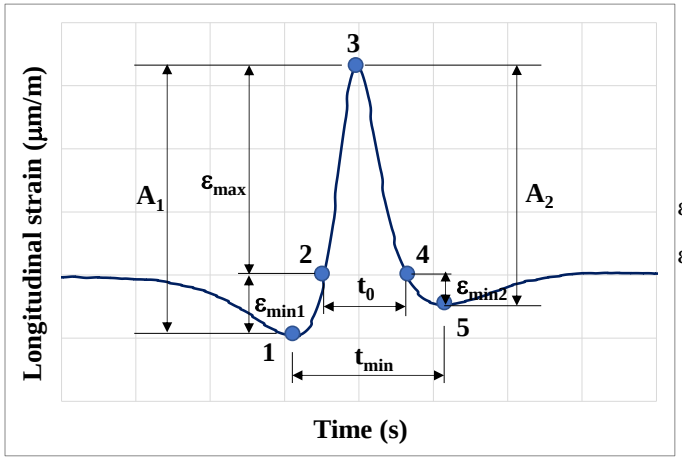

1,5 - Contraction points
2,4 - Zero points
3 - Tension point
ε_{max} - Maximum strain
ε_{min1} - Minimum strain 1
ε_{min2} - Minimum strain 2
A_1 - Strain amplitude (ε_{max} - ε_{min1})
A_2 - Strain amplitude (ε_{max} - ε_{min2})
t_0 - Time distance between zero points
t_{min} - Time distance between contraction points

Figure 7. Fundamental representations of a longitudinal strain signal.

In order to analyse the evolution of the longitudinal strain signal with traffic solicitations and temperatures, the following parameters are proposed:

In vertical axis (strain value):

- ε_{max}: the maximum longitudinal strain in extension,
- ε_{min1}: the minimum longitudinal strain in contraction (vertical distance between first contraction pick (1) and zero point (2)),
- ε_{min2}: the minimum longitudinal strain in contraction (vertical distance between second contraction pick (5) and zero point (4)),
- A_1: the strain amplitude (vertical distance between first contraction pick (1) and tension pick (3)),
- A_2: the strain amplitude (vertical distance between second contraction pick (5) and tension pick (3)).

In horizontal axis (time value):

- t_0: the time distance between two zero points (2,4),
- t_{min}: the time distance between two contraction points (1,5).

3.2. Effect of traffic solicitations and temperatures

On asphalt strain

According to the proposed parameters of a longitudinal strain signal in section 3.1, the two strain amplitudes (A_1, A_2) are employed to examine the effect of traffic solicitations and asphalt temperatures on the strain signal.

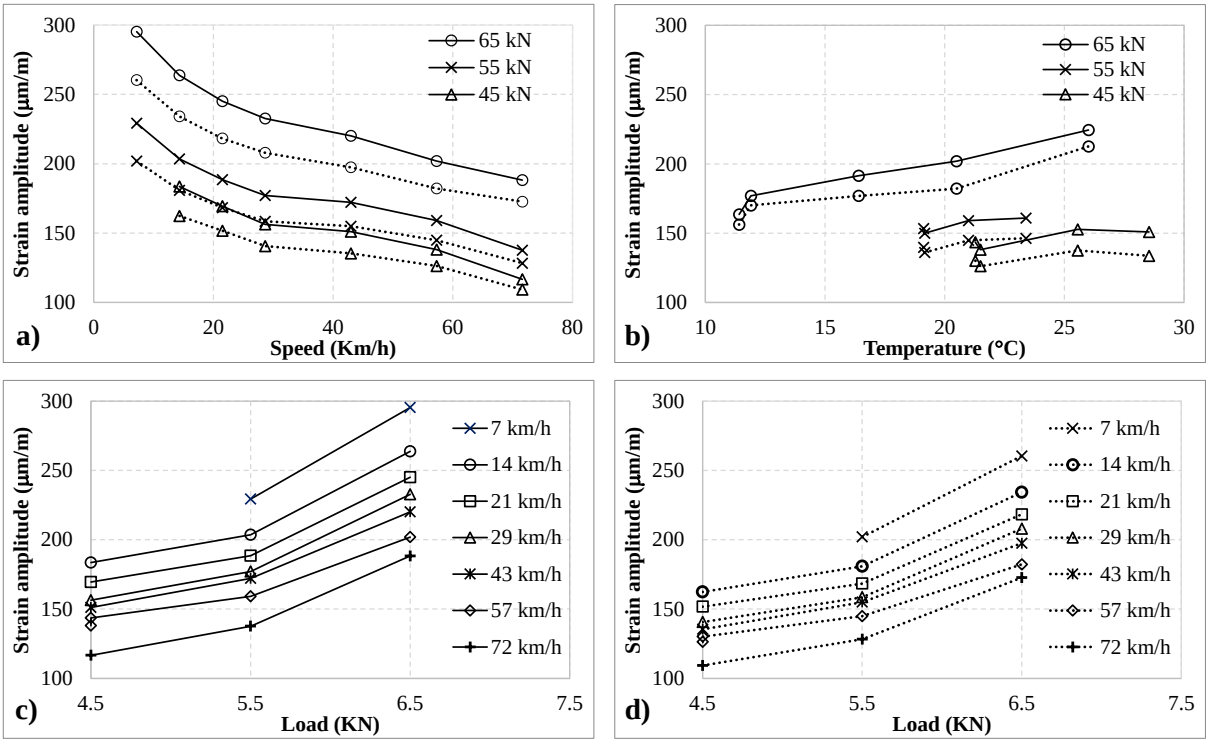

Figure 8. Effect of a) Traffic speed at 21°C, b) Asphalt temperature at the speed of 57 km/h, c) and d) Traffic load at 21°C to the tensile strain amplitude A_1 (Solid lines) and A_2 (Dotted lines).

Figure 8 shows the results of the experimental study, in which strain amplitudes between maximum pick of strain and first minimum pick (A_1 – solid lines), and second minimum pick (A_2 – dotted lines) over a range of traffic speeds (Figure 8a), asphalt temperatures (Figure 8b), and traffic loads (Figure 8c and Figure 8d). The figures indicate that strain response is affected by the change of those parameters, and the evolutions follow non-linear relationships. Concerning load levels, it can be observed from Figure 8 that the higher load level was, the higher strain amplitudes were at the same traffic speed and asphalt temperature condition. In the view of traffic speeds, the evolutions in Figures 8a, c, and d pointed out that with the increase of speed, the strain amplitudes (A_1 and A_2) decreased. This was mainly due to the increase of asphalt complex modulus at higher traffic speeds. The same observation was found in Figure 8b but with the decrease of asphalt temperature. The results in Figures 8c and 8d show that the non-linear relationships between the strain and load amplitude can be observed for rather small strain amplitude (less than 250 µm/m) [21,22]. Moreover, the differences are always observed when comparing the evolutions of the two strain amplitudes (A_1, A_2) in the same condition of traffic speed, traffic load, and temperature. Those observations validate the viscoelastic behaviour of asphalt material under the effect of traffic and temperature.

In the time domain

All the experimental strain responses in the study were time-based signals. Therefore, it is necessary to examine the evolution of the response time with all the inputs of loading and temperature. As proposed in Section 3.1, the two parameters t_0 and t_{min} are employed to serve as the assessment of asphalt tensile strain at different traffic speeds, traffic loads and asphalt temperatures.

Figure 9 shows the evolutions of parameters t_0 (dotted lines) and t_{min} (solid lines) with traffic speeds, asphalt temperatures, and traffic loads. It can be observed that the traffic loads (see Figure 9c and Figure 9d) and asphalt temperatures (see Figure 9b) have no significant effect on the tensile strain signal. Meanwhile, traffic speeds (see Figure 9a) modified the two parameters t_0 and t_{min}, particularly in the low-speed range (up to 30 km/h).

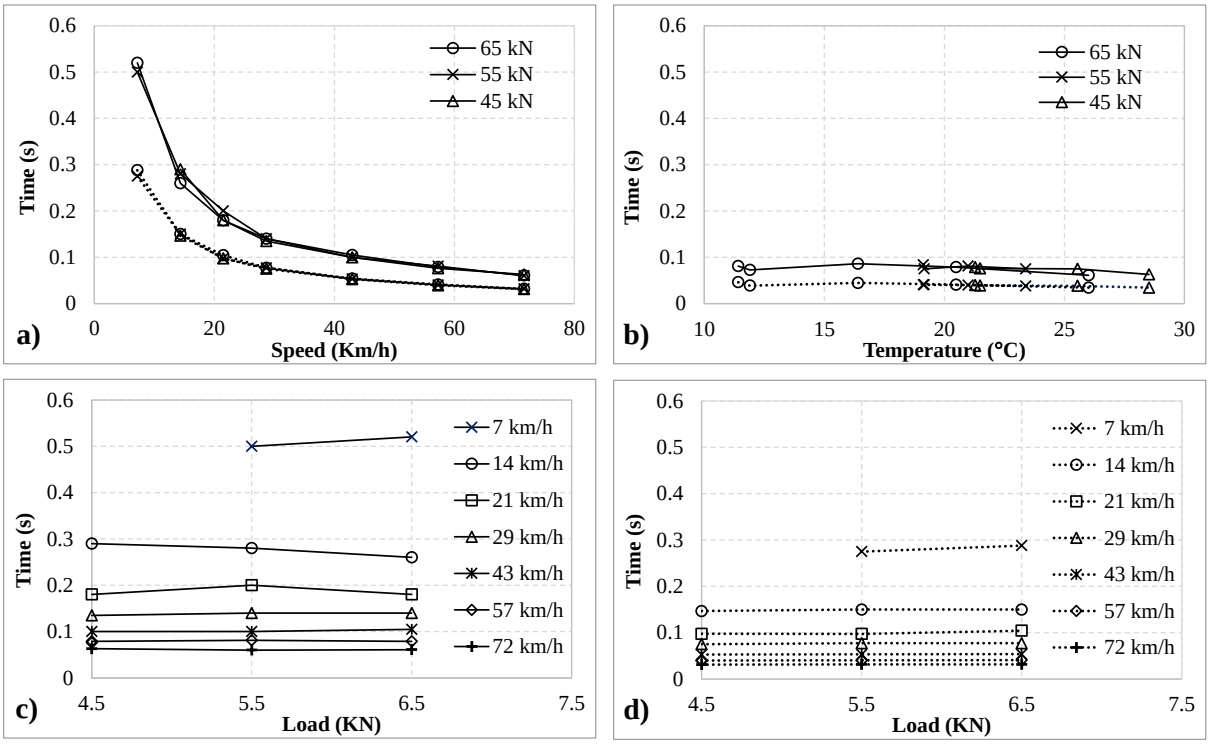

Figure 9. Effect of a) Traffic speed at 21°C, b) Asphalt temperature at the speed of 57 km/h, c) and d) Traffic load at 21°C to the time distance t_{min} (Solid lines) and t_0 (Dotted lines) of the strain signal.

3.3. Numerical simulation of the strain signal

The theoretical responses of the flexible pavement systems under the traffic load have been widely studied. Plenty of models were then developed to integrate those responses. For that purpose, there have been mainly two approaches that are used. The first approach has based on layered elastic theory, in which each pavement layer is homogenous, isotropic, and linear elastic [23,24]. This approach simplified the pavement structure into a two-dimensional (2D) model to calculate stresses, strains, and deflections in pavement layers. The second approach has based on the theory of the viscoelasticity of the pavement layers system, whereby three-dimensional (3D) responses of the pavement have been largely investigated [3,25,26].

In this study, numerical simulations of the strain signal will be introduced using Alize pavement design software [27] and ViscoRoute [28–30] for those static 2D and dynamic 3D models respectively. Following input data will be used:

- The simulations will be carried out with experimental conditions (pavement structure, traffic speed of 57 km/h, traffic load of 65 kN) for linear elastic and viscoelastic models with experimental asphalt temperature of 21°C. The pavement layers properties were summarized in Table 1.
- With regards to the thickness of the strain gauges (around 1.0 cm), the simulations will calculate the results at 0.5 cm from the bottom of the base asphalt layer where it is assumed that the experimental strain signals are obtained from strain gauges.
- For the simulation with Alize: The asphalt modulus data, which will be put in the material library of the program, is obtained from complex modulus tests in the laboratory [13]. The equivalent frequency at the traffic speed of 57 km/h is approximately 7.5 Hz according to the procedure presented in the parametric study of Bodin [31]. The frequency is then used to get the asphalt modulus in the simulation.
- For the simulation with ViscoRoute: The asphalt temperatures of 21°C and traffic speed of 57 km/h are used.

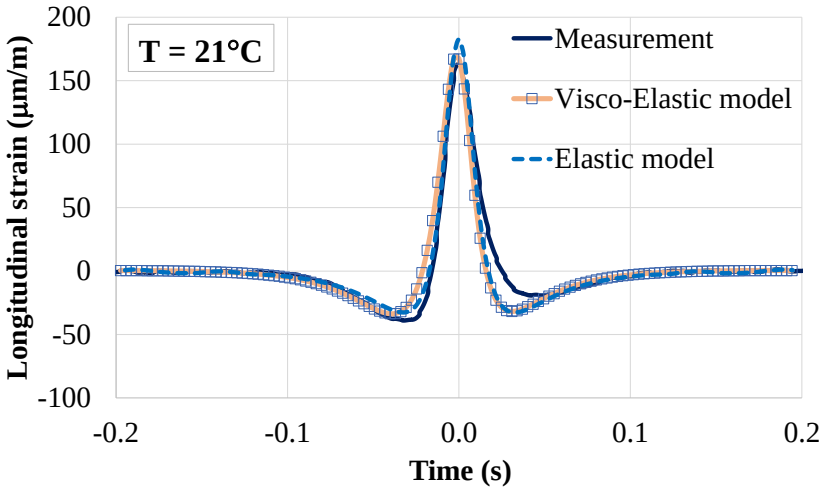

Figure 10. Measured and simulated (with elastic and viscoelastic models) longitudinal strains at V = 57 km/h, dual wheel of the axle loaded at 65 kN, 0.5 cm at the bottom of the asphalt layer for the temperature of 21°C.

The longitudinal strain signal comparison of measurement with elastic (Alize) and viscoelastic (ViscoRoute) simulations in Figure 10 (T = 21°C) indicates that both elastic and viscoelastic models give a good agreement with the measured strain signal. The simulated strain signals followed very well experimental one with regards to the shape and the peak values. The dissymmetry of the experimental signal could come from the imperfect strain gauge installation during the construction.

Table 1. Pavement layers properties for the simulations at the traffic speed of 57 km/h, asphalt temperature of 21°C, under the traffic load of 65 kN.

Pavement layer		Linear Elastic	Linear Viscoelastic
Asphalt concrete	Modulus (MPa)	8 093[1] (21°C, 7.5 Hz)	E^*[2] (21°C, 57 km/h)
	Thickness (cm)	11.5[3]	
UGM	Modulus (MPa)	190	
	Thickness (cm)	30	
Soil	Modulus (MPa)	100	
	Thickness (cm)	260	
Concrete substratum	Modulus (MPa)	55 000	

[1] *Obtained from the material library of the programme, with parameters from the complex modulus test [13].*

[2] *E* = 8 487 MPa, corresponding to traffic speed of 57 km/h, asphalt temperature of 21℃.*

[3] *Actual thickness of the two asphalt layers, measured by levelling measurement during the pavement construction.*

4. CONCLUSION

This paper presents an example of an experimental strain signal study in a full-scale pavement test to characterize a typical longitudinal strain signal at the bottom of the base asphalt layer. Strain signal parameters are introduced to follow the evolution of a signal under the accelerated dual wheel load. The traffic speed and traffic load were adjusted to obtain strain responses at respective asphalt temperatures. The examined results then pointed out that:

- The strain amplitudes were affected by the change of traffic solicitation levels and asphalt temperature. The non-linear relationships between those studied parameters could be explained by the viscoelastic behaviour of the asphalt material.
- In time domain: the two studied parameters t_0 and t_{min} were almost unchanged with different traffic load levels and asphalt temperatures while significant evolutions of those parameters were observed with the change of the traffic speed.

Numerical simulations of the strain signal with elastic and viscoelastic models are also presented in this study. The good agreement between modelled and experimental signals verified the applicability of those models to further studies.

The presented procedure has proved pavement instrumentation could serve as a suitable implement to measure and predict the pavement responses to loading for different types of researches in particular for parametric studies.

ACKNOWLEDGMENT

Part of the experimental data presented in this paper comes from the full-scale test of the ANR SolDuGri project (ANR-14-CE22-0019). This research is funded by University of Transport and Communications (UTC) under grant number T2021-CT-030.

REFERENCES

[1]. J. F. Corte, M. T. Goux, Design of Pavement Structures - The French Technical Guide: Journal of the Transportation Research Board, 1539 (1996) 116-124. https://doi.org/10.1177/0361198196153900116
[2]. H. L. Theyse, M. De Beer, F. C. Rust, Overview of South African Mechanistic Pavement Design Method: Journal of the Transportation Research Board, 1539 (1996) 6-17. https://doi.org/10.1177/0361198196153900102
[3]. Y. H. Huang, Pavement analysis and design: Upper Saddle River, Pearson/Prentice Hall, 2004.
[4]. J. Blanc, P. Hornych, Z. Sotoodeh-Nia, C. Williams, L. Porot, S. Pouget, R. Boysen, J. P. Planche, D. L. Presti, A. Jimenez, E. Chailleux, Full-scale validation of bio-recycled asphalt mixtures for road pavements: Journal of Cleaner Production, 227 (2019) 1068–1078. https://doi.org/10.1016/j.jclepro.2019.04.273
[5]. H. Cheng, J. Liu, L. Sun, L. Liu, Critical position of fatigue damage within asphalt pavement considering temperature and strain distribution: International Journal of Pavement Engineering, (2020) 1-12. https://doi.org/10.1080/10298436.2020.1724288
[6]. M. L. Nguyen, O. Chupin, J. Blanc, J. M. Piau, P. Hornych, Y. Lefeuvre, Investigation of Crack Propagation in Asphalt Pavement Based on APT Result and LEFM Analysis: Journal of Testing and Evaluation, 48 (2020) 20180933. https://doi.org/10.1520/JTE20180933
[7]. M. H. Shafiee, L. Hashemian, A. Asefzadeh, A. Bayat, Time–Frequency Domain Analysis of Asphalt Longitudinal Strain: Journal of the Transportation Research Board, 2590 (2016) 56-64. https://doi.org/10.3141/2590-07
[8]. P. J. Yoo, I. L. Al-Qadi, M. A. Elseifi, I. Janajreh, Flexible pavement responses to different loading amplitudes considering layer interface condition and lateral shear forces: International Journal of Pavement Engineering, 7 (2006) 73-86. https://doi.org/10.1080/10298430500516074
[9]. I. L. Al-Qadi, A. Loulizi, M. Elseifi, S. Lahouar, The Virginia Smart Road: The Impact of Pavement Instrumentation on Understanding Pavement Performance: Asphalt Paving Technology: Association of Asphalt Paving Technologists-Proceedings of the Technical Sessions, 73 (2004) 427-465.
[10]. NF EN 13108-1, Bituminous mixtures - Material specifications - Part 1: Bituminous mixes, in French, 2007.
[11]. EN 12591, Bitumen and bituminous binders - Specifications for paving grade bitumens: Comite Europeen de Normalisation, 2009.
[12]. NF P94-117-2, Soils: investigation and testing - Formation level bearing capacity - Part 2: Dynamic deformation module, French standard, 2004.
[13]. EN 12697-26, Bituminous Mixtures - Test Methods for Hot Mix Asphalt - Part 26: Stiffness, London, UK: British Standards Institution, 2018.
[14]. J. F. Corte, H. Di Benedetto, Matériaux routiers bitumineux 1: description et propriétés des constituants: Hermes-Lavoisier, 2004.
[15]. Q. T. Nguyen, H. Di Benedetto, C. Sauzeat, N. Tapsoba, Time Temperature Superposition Principle Validation for Bituminous Mixes in the Linear and Nonlinear Domains: Journal of Materials in Civil Engineering, 25 (2013) 1181-1188. https://doi.org/10.1061/(ASCE)MT.1943-5533.0000658
[16]. M. L. Williams, R. F. Landel, J. D. Ferry, The Temperature Dependence of Relaxation Mechanisms in Amorphous Polymers and Other Glass-forming Liquids: Journal of the American Chemical Society, 77 (1955) 3701-3707. https://doi.org/10.1021/ja01619a008

[17]. M. L. Nguyen, J. Blanc, J. P. Kerzreho, P. Hornych, Review of glass fibre grid use for pavement reinforcement and APT experiments at IFSTTAR: Road Materials and Pavement Design, 14 (2013) 287-308. https://doi.org/10.1080/14680629.2013.774763
[18]. J. Blanc, E. Chailleux, P. Hornych, C. Williams, D. V. Presti, A. Jimenez, L. Porot, J. P. Planche, S. Pouget, Bio materials with reclaimed asphalt: from lab mixes properties to non-damaged full scale monitoring and mechanical simulation: Road Materials and Pavement Design, 20 (2019) 95-111. https://doi.org/10.1080/14680629.2019.1589557
[19]. I. Al-Qadi, Ed., Advances in Pavement Design through Full-scale Accelerated Pavement Testing: CRC Press, 2012. https://doi.org/10.1201/b13000
[20]. M. L. Nguyen, P. Hornych, M. Dauvergne, L. Lumière, C. Chazallon, S. Mouhoubi, M. Sahli, D. Doligez, E. Godard, Development of a rational design procedure based on fatigue characterisation and environmental evaluations of asphalt pavement reinforced with glass fibre grid: Road Materials and Pavement Design, 22 (2021) 672-689. https://doi.org/10.1080/14680629.2021.1906304
[21]. Q. T. Nguyen, H. Di Benedetto, C. Sauzéat, Linear and nonlinear viscoelastic behaviour of bituminous mixtures: Materials and Structures, 48 (2015) 2339-2351. https://doi.org/10.1617/s11527-014-0316-5
[22]. Q. T. Nguyen, M. L. Nguyen, H. D. Benedetto, C. Sauzeat, E. Chailleux, T. T. N. Hoang, Nonlinearity of bituminous materials for small amplitude cyclic loadings: Road Materials and Pavement Design, 20 (2019) 1571-1585. https://doi.org/10.1080/14680629.2018.1465452
[23]. J. Boussinesq, Application des potentiels à l'étude de l'équilibre et du mouvement des solides élastiques, principalement au calcul des déformations et des pressions que produisent, dans ces solides, des efforts quelconques exercés sur une petite partie de leur surface ou de leur intérieur: mémoire suivi de notes étendues sur divers points de physique mathématique et d'analyse: Impr Danel Lille, 1885.
[24]. D. M. Burmister, L. A. Palmer, E. S. Barber, T. A. Middlebrooks, The Theory of Stresses and Displacements in Layered Systems an d Applications to the Design of Airport Runways: Highway Research Board Proceedings, 1943.
[25]. S. P. Timoshenko, J. N. Goodier, Theory of Elasticity: Mcgraw-Hill Education, 1951.
[26]. A. Ahmed, S. Erlingsson, Viscoelastic Response Modelling of a Pavement under Moving Load: Transportation Research Procedia, 14 (2016) 748-757. https://doi.org/10.1016/j.trpro.2016.05.343
[27]. P. Autret, A. Baucheron de Boissoudy, J. P. Marchand, ALIZE III practice: Delft, Netherlands, 1982.
[28]. A. Chabot, O. Chupin, L. Deloffre, D. Duhamel, ViscoRoute 2.0 A: Tool for the Simulation of Moving Load Effects on Asphalt Pavement: Road Materials and Pavement Design, 11 (2010) 227-250. https://doi.org/10.1080/14680629.2010.9690274
[29]. O. Chupin, A. Chabot, J. M. Piau, D. Duhamel, Influence of sliding interfaces on the response of a layered viscoelastic medium under a moving load: International Journal of Solids and Structures, 47 (2010) 3435-3446. https://doi.org/10.1016/j.ijsolstr.2010.08.020
[30]. O. Chupin, J. M. Piau, A. Chabot, Evaluation of the structure-induced rolling resistance (SRR) for pavements including viscoelastic material layers: Materials and Structures, 46 (2013) 683-696. https://doi.org/10.1617/s11527-012-9925-z
[31]. D. Bodin, O. Chupin, E. Denneman, Viscoelastic Asphalt Pavement Simulations and Simplified Elastic Pavement Models Based on an 'Equivalent Asphalt Modulus' Concept: Journal of Testing and Evaluation, 45 (2017) 20160652. https://doi.org/10.1520/JTE20160652